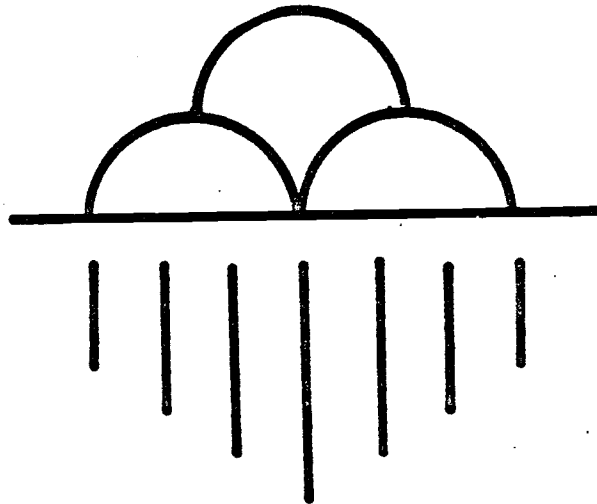


CASE STUDY SIMULATIONS OF DRY WELL DRAINAGE  
IN THE TUCSON BASIN

By

Reid F. Bandeen  
Water Resources Research Center  
College of Engineering  
University of Arizona  
Tucson, Arizona 85721



Completion Report to  
Pima County Transportation and Flood  
Control District

SEPTEMBER 1984

### Acknowledgements

This project was supported in part by the following agencies:

Pima County Department of Transportation and  
Flood Control District

State of Arizona

U. S. Department of Interior, Geological Survey

The author gratefully acknowledges the assistance of the following individuals:

L. G. Wilson, Acting Director of the Water Resource Research Center, University of Arizona and principal investigator of this project, for his assistance and guidance throughout the project.

Dr. Shlomo Neuman, Department of Hydrology and Water Resources, University of Arizona, for his invaluable assistance in the modeling phases of this study.

S. DeTommaso, McGuckin Drilling Co., Tucson, Arizona, for providing information on the design and function of dry wells.

Cella Barr Associates, Consulting Engineers, Tucson, Arizona, for providing information on simulation of storm runoff.

Brenda Keller, University of Arizona Computer Center, for assistance in performing computer runs.

TABLE OF CONTENTS

	<u>Page</u>
Introduction. . . . .	1
Case Studies. . . . .	3
Case 1a. . . . .	6
Case 1b. . . . .	6
Case 2a. . . . .	9
Case 2b. . . . .	9
Procedure . . . . .	9
a. Program Unsat 2. . . . .	9
b. Flow Grid. . . . .	9
c. Model Inputs . . . . .	12
d. Determination of Soil Hydraulic Properties . . . . .	13
1. Saturated Hydraulic Conductivity . . . . .	13
2. Pressure Head as Function of Water Content . . . . .	19
3. Unsaturated Hydraulic Conductivity . . . . .	19
Discussion of Results . . . . .	24
Case 1a. . . . .	24
Case 1b. . . . .	24
Case 2a. . . . .	27
Case 2b. . . . .	27
Conclusions and Recommendations . . . . .	32
Sources and References. . . . .	33

TABLES

<u>Number</u>	<u>Subject</u>	<u>Page</u>
1	Infiltration Test Data. . . . .	15
2	Calculated $K_s$ Values. . . . .	17
3a	Moisture Retention Data for Material 2. . . . .	22
3b	Relative Hydraulic Conductivity Data for Material 2. . . . .	23
4	Cumulative Inflow Data. . . . .	31

FIGURES

<u>Number</u>	<u>Title of Figure</u>	<u>Page</u>
1	Typical Dry Well Design. . . . .	2
2	Conceptualized Cross-Section of Vadose Zone at Dry Well Site. . . . .	5
3	U.S. Soil Conservation Service Triangular Unit Hydrograph . . . . .	7
4	SCS Hydrograph for 100-Year, 1 Hour Storm in Tucson Area . . . . .	8
5	Example Two-Dimensional Flow Grid for Program Unsat 2. . . . .	10
6	Representation of Axisymmetric Flow Region by Rectangular Grid . . . . .	11
7	Derivation of $\alpha$ from $\log K_r$ vs $-\Psi$ Curve . . . . .	14
8	Plot of Flow Rate vs $t^{-1/2}$ for Derivation of Saturated Hydraulic Conductivity . . . . .	16
9a	Experimentally Derived $\Psi$ vs $\theta$ Curve. . . . .	20
9b	$K_r$ vs $\theta$ Curve for Material 1 . . . . .	21
10	Flow Profile for Case 1a . . . . .	25
11	Flow Profile for Case 1b . . . . .	26
12a-c	Flow Profile for Case 2a . . . . .	28-30

## Introduction

Recent rapid growth in the Southwest and other parts of the country has led to an escalation of the problem of urban runoff. As land development proceeds, increased paved area in a given community often creates storm water runoff volumes that overload existing routing and detention/retention capabilities. In Arizona, many community governments have passed legislation requiring new developments to be provided with detention/retention schemes to handle any additional runoff resulting for downstream areas. The recent approval of an amendment to the Floodplain Management Ordinance by the Pima County Board of Supervisors requiring emplacement of appropriate detention/retention facilities in certain watersheds deemed to be in danger of increased flood risk due to further development is a good example.

A relatively new, but already widely used innovation in storm water retention is the "dry well," a structure that allows for rapid channeling of flood water from the ground surface into permeable sediments beneath. Although the dry well is widely acknowledged as a very effective means of flood water disposal, concern that pollutants in runoff water, and perhaps other waste water channeled into dry wells, may eventually degrade underlying ground water supplies has slowed its acceptance in Pima County. The Pima County Floodplain Management Ordinance stipulates that

The effects of recharging storm runoff and possible pollution of ground water should be evaluated for all systems employing infiltration systems, such as dry wells, in order to prevent contamination of the ground water.

One of the principal ways a dry well could contaminate ground water would be via leakage of fresh, possibly contaminated runoff to the aquifer by way of the highly conductive zone immediately surrounding the bore of a water supply well. Due to abrupt changes in the permeability of vadose zone sediments, water draining from a dry well may "perch" temporarily atop a layer of lesser permeability, and undergo significant lateral movement. If sufficient water were introduced into the dry well

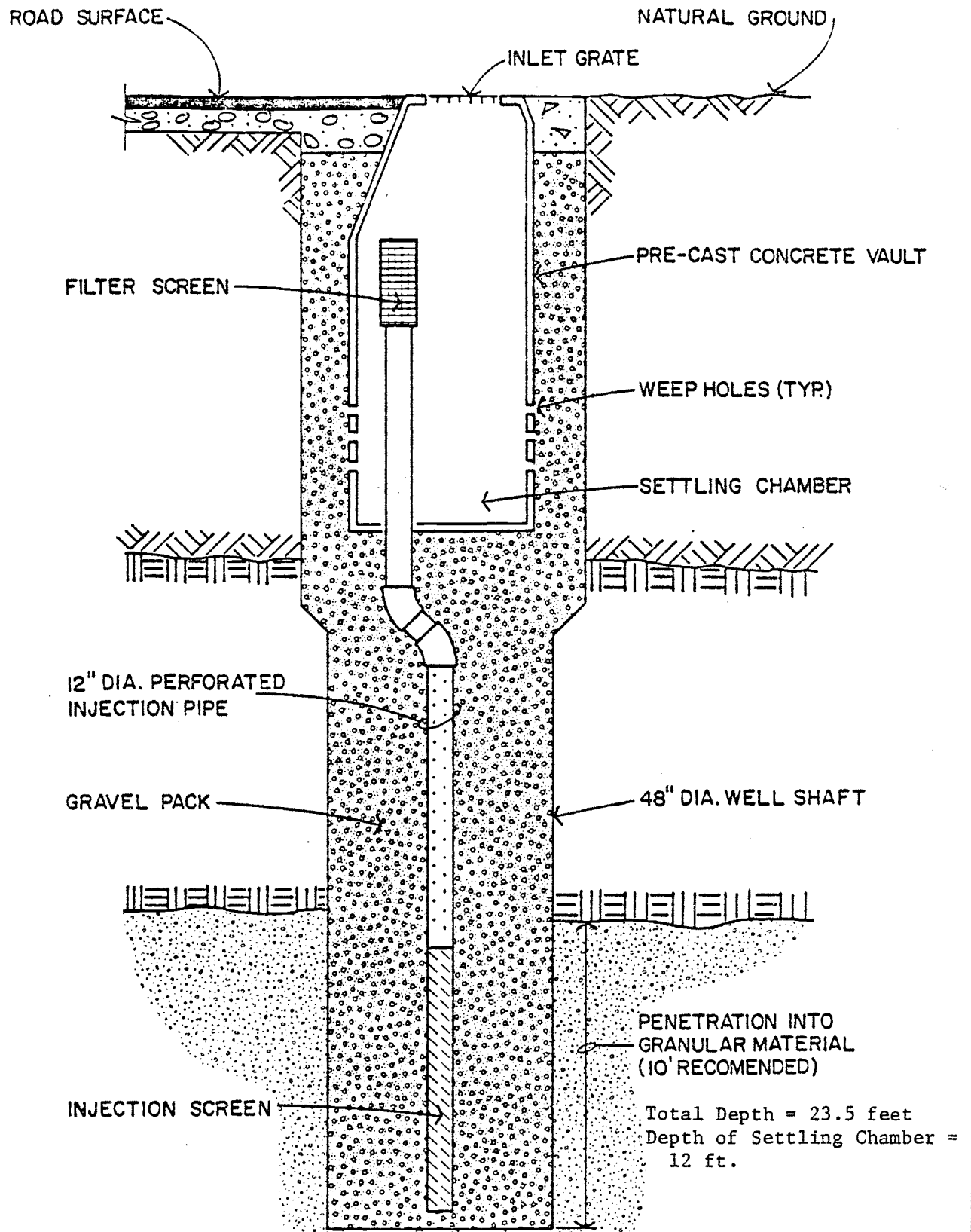


**FIGURE 1**  
**TYPICAL DRYWELL DESIGN** (after Camp Dresser & McKee, Inc.)  
**NO SCALE**

over a short enough time, enough lateral migration could occur for that water to reach a well bore, where it may drain directly to the aquifer through the highly permeable gravel pack or disturbed zone surrounding the casing, or through cracks in the casing itself (Campbell & Lehr, p. 18). Given that runoff routed to dry wells will frequently be coming from paved areas surrounding commercial and industrial areas where normal operations or accidental spillage may lead to dangerously high levels of pollutants in runoff water, together with the fact that water moving laterally and leaking through a well bore will benefit much less from the natural filtering processes of the soil than water draining vertically hundreds of feet before reaching the aquifer, concern for potential pollution is justified. This concern could be allayed, however, were dry wells emplaced a sufficient distance from any nearby water supply wells to insure that any laterally moving perched water could not extend so far as to reach a well bore. Thus we are in need of establishing some design criteria for dry wells regarding their placement relative to water wells to ensure their safe use. The objective of this study is to provide experimental data from field tests and computer simulations performed on an experimental dry well located at the University of Arizona Water Resource Research Center (WRRC) Field Laboratory that may serve as a basis for establishing these design criteria, and provide recommendations as such. The results of a separate study of the fate of selected contaminants contained in simulated urban runoff performed on the same experimental dry well have already been published (Wilson, 1983). An illustration of the Max Well Type III dry well made by McGuckin Drilling Co. used in this study is shown in Figure 1. For more information on the design and construction of this dry well the reader is referred to the 1983 study by Wilson, listed as a reference.

### Case Studies

Dry wells serve to aid drainage of storm water in two principal ways: 1) to directly dispose of local runoff from a given rainfall/runoff event, and 2) to dispose of a larger volume of stored water, such as that from a detention reservoir, over a longer period of time. During the computer simulation phase of the study, two separate inflow



regimes were used as input: a) simulated runoff from a design flood used by Pima County as a standard for testing the feasibility of flood prevention schemes, to address case 1 above, and b) sustained inflow to a dry well at a given design flow rate specified by the dry well manufacturer to simulate the second case of longer term drainage of stored water.

Two distinct subsurface flow regimes were also considered. Permeability and depth below ground of perching strata will vary throughout the Tucson basin. The scope of this study is confined to simulating dry well drainage under subsurface conditions at the WRRRC Field Laboratory, which may be regarded as typical of the Tucson basin, though certainly not exactly representative of subsurface conditions everywhere in the basin. Here the depth of the perching layer was determined, through analysis of neutron moisture logs obtained during tests of the dry well, to be approximately 32 feet below the ground surface. The two subsurface flow regimes simulated were 1) perching layer of zero permeability, and 2) perching layer composed of material having finite permeability considerably less than that of the overlying alluvium. The first case above was meant to be used as a "worst possible case," for when no vertical leakage takes place through the perching layer, lateral movement of drained water along this layer will be at a maximum. The assumption of a totally impermeable perching layer would be realistic only in the presence of a locally continuous layer of caliche, a rock-like material formed by the cementation of gravelly sand by percolating calcium carbonate-bearing ground water solutions. These layers vary widely in depth, thickness and continuity within the Tucson basin. Depth may vary from less than five to several feet. The layers may be discontinuous, existing only in localized patches, or be continuous over an area of several acres (Heckman, 1984). Clearly, these layers may facilitate subsurface lateral flow. Many perched zone monitor wells are designed to terminate in a layer of caliche (Heckman, 1984). Locally pure and continuous clay layers may have very nearly zero permeability, and can also act as a base for maximum lateral flow. The second case represents the more common

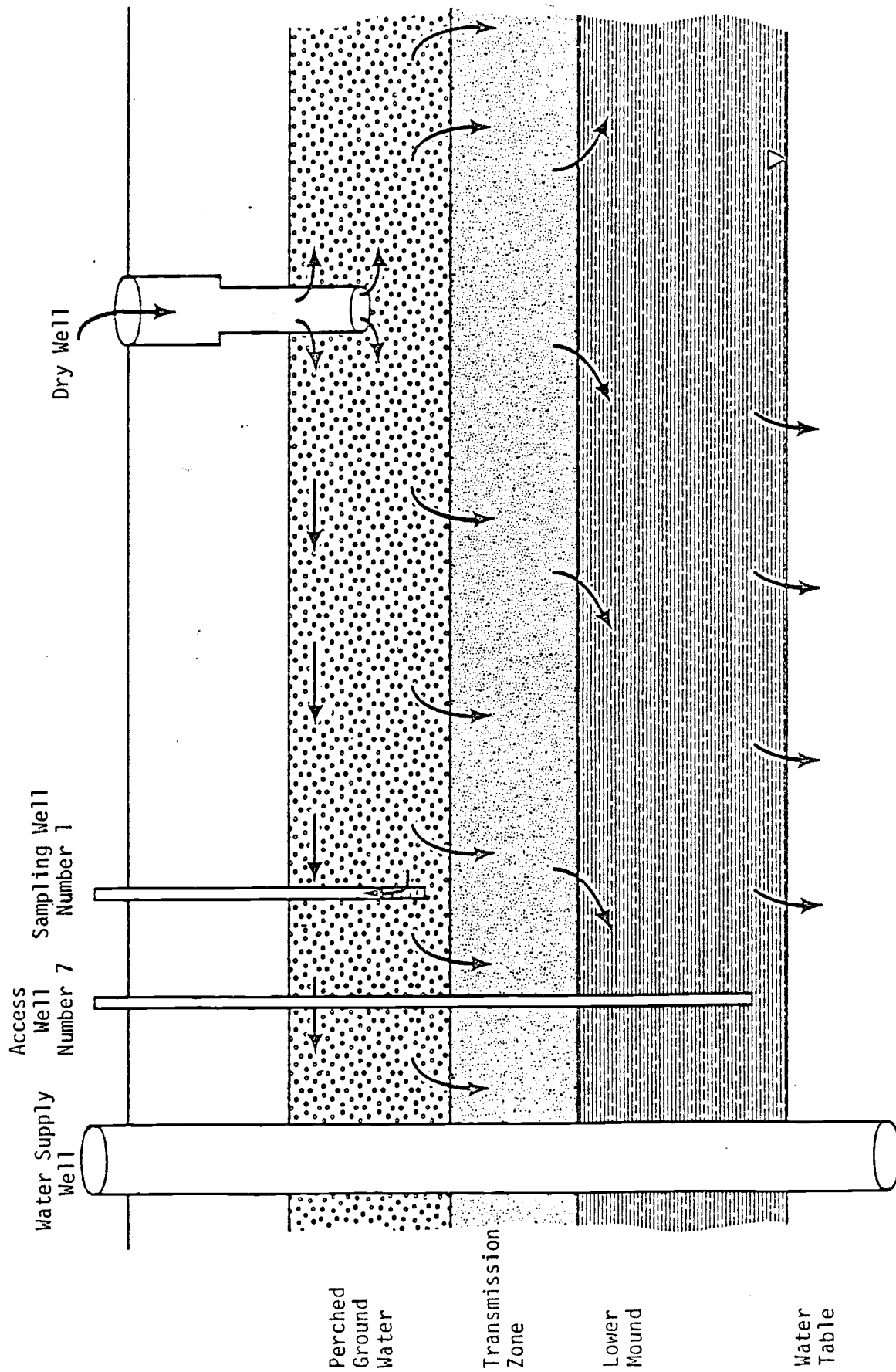


FIGURE 2. Conceptualized Cross-Section of Vadose Zone at Dry Well Site, Showing Flow Paths During Injection. (After Wilson, 1983).

situation of the perching layer being much less permeable than overlying material, still allowing for some vertical drainage of water along with the perching and lateral movement caused by the abrupt change in permeability between the two materials. Figure 2 shows a conceptual cross section of dry well drainage. The "perching layer" referred to previously is pictured here as the "transmission zone." This layer will be assigned zero or finite permeability depending on the simulation. The two inflow regimes were combined with the two subsurface flow regimes to produce the four case studies discussed below.

Case 1a: Localized Drainage of Runoff from  
Design Storm; Lateral Flow with No  
Vertical Leakage.

Here runoff from a 100-year, 1-hour storm event, the design flood used in most flood management schemes by the Pima County Floodplain Management District (Nelson, 1984), was simulated using a hydrograph method created by the U.S. Soil Conservation Service (SCS) in conjunction with a subsurface flow regime featuring an impermeable perching stratum. Runoff for the 100-year, 1-hour storm was calculated from the SCS triangular hydrograph shown in Figure 3, using the following parameters derived for the Tucson basin from meteorological data (Nelson, 1984):

$$T_p = 0.23 \text{ hrs.}$$

$$T_r = (1.7)T_p = 0.39 \text{ hrs.}$$

$$T_b = 0.62 \text{ hrs.}$$

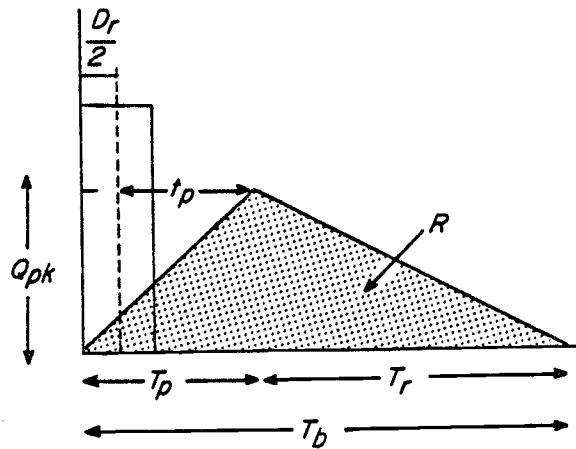
$$Q_p = 8.57 \text{ in/hr.}$$

These figures correspond to the expected runoff from a single paved acre, the design service area of a single dry well specified by the manufacturer (DeTomasso, 1984). Using these parameters allows for the construction of the hydrograph in Figure 4, which indicates a total runoff volume of 9644 cubic feet.

Case 1b: Localized Drainage of Runoff from  
Design Storm; Lateral Flow with  
Vertical Leakage.

Here the inflow regime is the same as that above, only the perching layer is assumed to be composed of a separate material of lesser

$$R = \frac{Q_{pk} T_p}{2} + \frac{Q_{pk} T_r}{2}$$



- $R$  = volume of storm runoff (in.)  
 $Q_{pk}$  = peak rate of runoff (in/hr.)  
 $T_p$  = time of rise to peak (hr.)  
 $T_r$  = duration of recession limb (hr.)  
 $T_b$  = time base or duration of rainfall excess

Figure 3. U.S. Soil Conservation Service Triangular Unit Hydrograph (after Dunne and Leopold, p. 342).

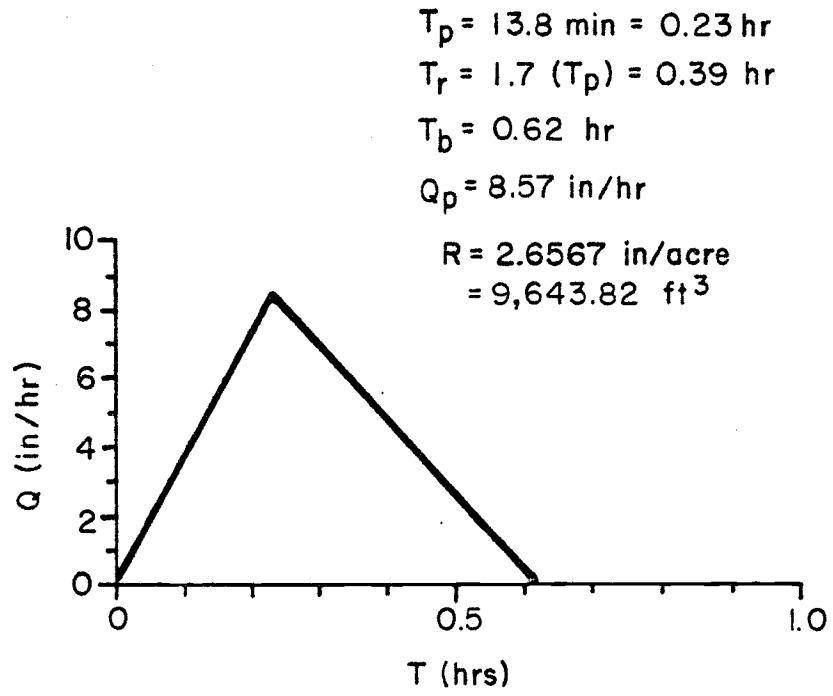


Figure 4. SCS Hydrograph for 100-year, 1-hour storm in the Tucson Area.

permeability. Information obtained from logs kept from previous drilling operations at the WRRRC Field Lab was used to derive a distinct set of hydraulic properties for this material. The upcoming section subtitled "Determination of Hydraulic Properties" offers a more complete explanation of how these properties were derived.

Case 2a: Steady-State Drainage of Stored Runoff;  
No Vertical Leakage

This simulation was made to address the case where a dry well is used to drain large amounts of stored water over longer periods of time. A steady flow rate of 0.5 cubic feet per second, the expected long-term performance flow rate specified by the manufacturer (DeTomaso, 1984), was used in this phase of the simulation, over a period in excess of the 24-hour maximum drainage time for flood water detention areas proposed in Pima County Floodplain Management Ordinance 1974-86, Section 1307. Here again the assumption is made of an impermeable perching stratum.

Case 2b: Steady-State Drainage of Stored Runoff  
with Vertical Leakage.

This case is essentially the same as case 2a, only the perching layer is assumed to have a finite permeability determined by the hydraulic properties described under case 1b.

Procedure

a. Program Unsat 2

Computer simulation of subsurface flow from a dry well for the cases described previously was performed using Program Unsat 2, developed largely by Dr. Shlomo Neuman of the University of Arizona to simulate problems of nonsteady seepage in saturated-unsaturated porous media. The program utilizes the Galerkin method in conjunction with a finite element discretization scheme to deal with two-dimensional or axisymmetric three dimensional flow problems.

b. Flow Grid

Use of the model requires the construction of a two dimensional "grid" of "flow cells," which represents the porous medium (see Figure 5).

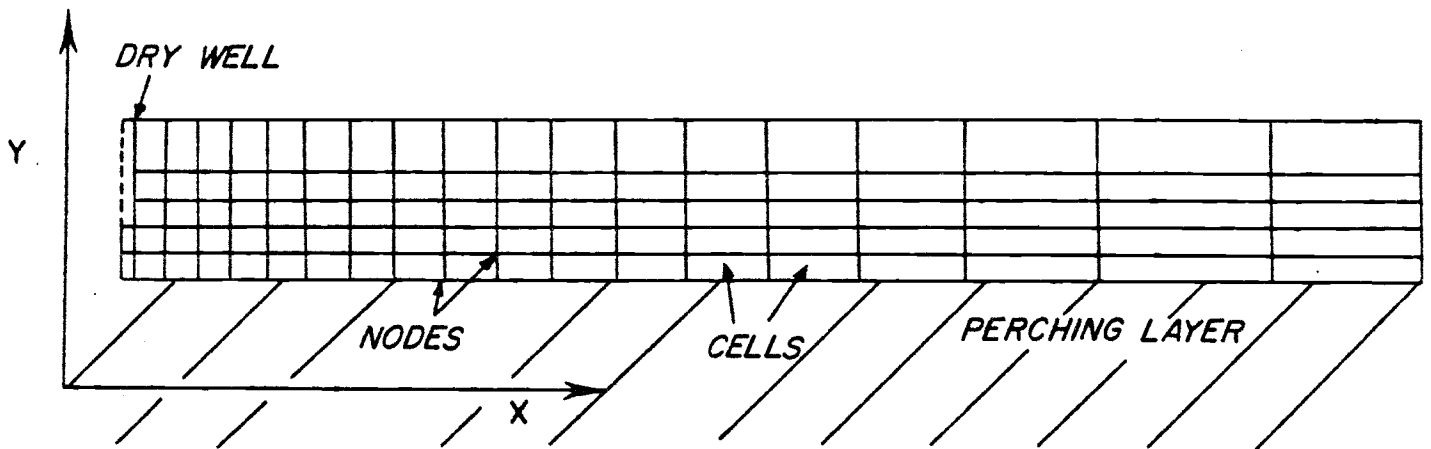


Figure 5. Example Two-Dimensional Flow Grid for Program Unsat 2.

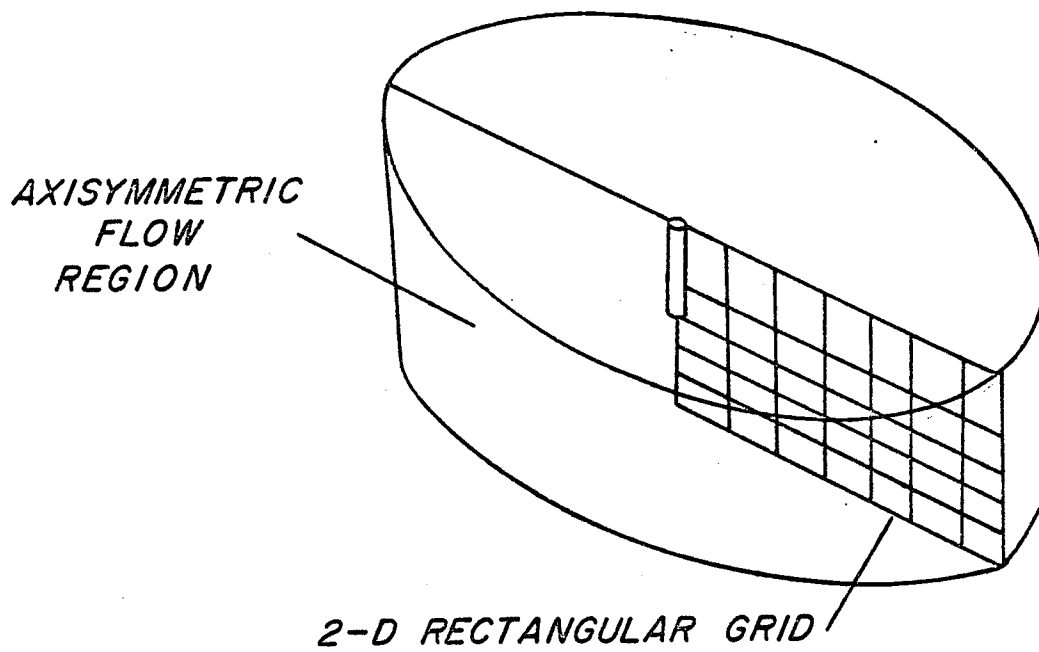


Figure 6. Representation of Axisymmetric Flow Region by Rectangular Grid.



The intersection points of the grid lines are called "nodes." The dry well "source" is represented by the rectangular indentation at the upper left side of the Figure 5 grid. Here the dry well is represented essentially as a borehole of depth 23.5 feet and radius of 2 feet, the area which includes the gravel packing around the dry well. As the dry well chamber is perforated up to a level of about 8.25 feet below ground surface, the dry well can be treated for simulation purposes as a gravel-filled borehole up to this level. Incoming flow to the system is simulated either by imposing a prescribed volume flux for the nodes bordering the dry well, or assigning a hydraulic head value for each of these nodes which remains constant throughout the simulation. This flow problem is one of the "axisymmetric," or radial flow type, where the entire flow region, obtained by rotating the two-dimensional grid  $360^\circ$  about its axis at the dry well source is represented to the program by the two-dimensional grid section (see Figure 6). As flow is introduced into the grid, the program proceeds to iterate over a number of "time steps" of specified length, giving as output the hydraulic and pressure head values calculated for each node at the end of each time step. From this information, a "profile" of the saturated zone may be constructed within the grid, and its rate of movement derived by comparing profiles between time steps.

#### c. Model Inputs

The resultant flow regime predicted by the model depends largely on certain input parameters stored by the program depicting the hydraulic properties of the porous medium. These are 1) saturated hydraulic conductivity or  $K_s$ , 2) a functional relation between relative hydraulic conductivity, the ratio of a given unsaturated hydraulic conductivity and the  $K_s$  value (ranging from 0 to 1), and water content,  $\theta$ , a measure of the volume of water contained per volume of soil, 3) a similar relation between the amount of suction, measured as a negative pressure head,  $-\Psi$ , which corresponds to a given volumetric water content. The  $K_s$  value was determined from a combination of data collected in the field and an analytical technique. The saturated hydraulic conductivity,  $K_s$ , is the fundamental constant in the model's saturated flow equation, and determines how fast water will flow through the porous medium under a

given hydraulic head gradient. The  $-\Psi$  vs  $\theta$  and  $K_r$  vs  $\theta$  relationships are used in describing unsaturated flow, and determine rate of water movement through an unsaturated soil under variable subsurface pressure and moisture conditions. The  $-\Psi$  vs  $\theta$  relationship was derived from the  $-\Psi$  vs  $\theta$  using a special analytical model derived for this purpose. The details of how these quantities were obtained are presented in the following section.

d. Determination of Soil Hydraulic Properties

1. Saturated Hydraulic Conductivity:

A method developed at the University of Arizona for the determination of saturated hydraulic conductivity from constant head borehole infiltration tests (Stephens & Neuman, 1980) was employed in this study. Using numerical simulations based on the observed unsaturated hydraulic properties of four different soils, these authors developed an empirical formula for the saturated hydraulic conductivity for an unsaturated soil that showed improved accuracy over older, more established methods. This formula is given as

$$\log C_u = 0.658 \log H_d - 0.238 \sqrt{\alpha} - 0.398 \log H + 1.343$$

$$C_u = Q_s / K_s r H$$

where  $Q_s$  = flow rate at steady state ( $m^3/day$ )

$r$  = borehole radius (m)

$H$  = height of water column in borehole (m)

$$H_d = H/r$$

$\alpha$  = average slope of (natural) log relative hydraulic conductivity vs pressure head curve over the range  $(0.5 \leq K_r \leq 1.0)$

Data from six infiltration tests performed at the WRRRC Field Lab were used with this formula to obtain a distribution of  $K_s$  values. A specific application of this formula is described below.

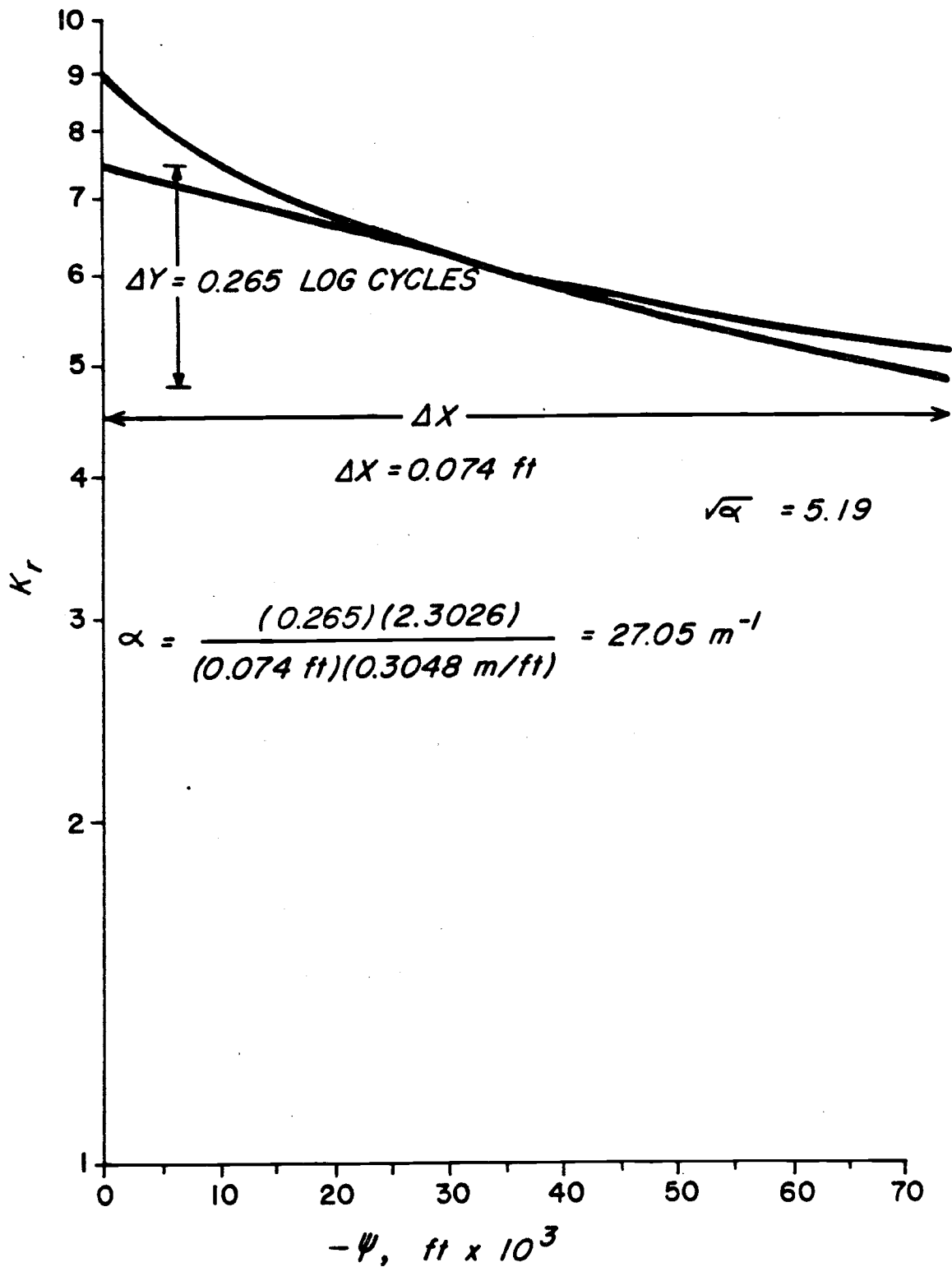


Figure 7. Derivation of  $\alpha$  from  $\log K_r$  vs  $-\Psi$  Curve.

TABLE 1: INFILTRATION TEST DATA

Elapsed time (min.)		Well Discharge (gpm)	Total AT T <sub>1</sub>	Head (ft.)	Specific Intake at t <sub>2</sub> (gpm/ft)	Additional Data
t <sub>1</sub>	t <sub>2</sub>					
0.0			--			Total Head(ft.)*
0.5			--			Head Constant =
6.0			6.92			4.416
7.0			7.17			Ave. Head =
8.0			7.42			5.414
9.0			7.67			Total 9.830
10.0			7.92			
11.0			8.08			
12.0			8.21			
13.0			8.25			*Measured from
14.0			8.54			bottom of well.
15.0	15.0	316.16	8.54	8.35	37.86	
16.0			8.67			
17.0			8.67			
18.0			8.71			
19.0			8.79			
20.0			8.88			
21.0			8.92			
22.0			8.96			
25.0			9.08			
30.0			9.25			
35.0			9.38			
40.0	45.0	307.02	9.42	9.45	32.48	
50.0			9.46			
55.0			9.63			
60.0			9.58			
75.0	75.0	306.15	9.67	9.65	31.71	
90.0			9.71			
105.0	105.0	305.58	9.67	9.70	31.51	
120.0	135.0	304.09	9.71	9.71	31.32	
150.0	165.0	305.86	9.71	9.72	31.47	
180.0	195.0	304.37	9.73	9.76	31.19	
210.0			9.79	9.76	31.19	
240.0	225.0	303.68	9.81	9.80	30.99	
270.0	255.0	302.86	9.81	9.81	30.87	
300.0	285.0	303.03	9.90	9.86	30.75	
330.0	315.0	303.56	9.85	9.88	30.74	
360.0	345.0	302.81	9.90	9.88	30.66	
390.0	375.0	301.71	9.85	9.88	30.55	
420.0	405.0	299.90	9.81	9.83	30.51	
450.0	435.0	298.77	9.83	9.82	30.43	
480.0	465.0	299.03	9.82	9.82	30.45	
510.0	495.0	298.47	9.77	9.77	30.55	
540.0	525.0	299.91	9.74	9.74	30.79	
570.0	555.0	297.24	9.75	9.75	30.49	
600.0	585.0	293.48	7.63			
600.5			7.13			
601.0			not			
601.5			measure-			
			able			

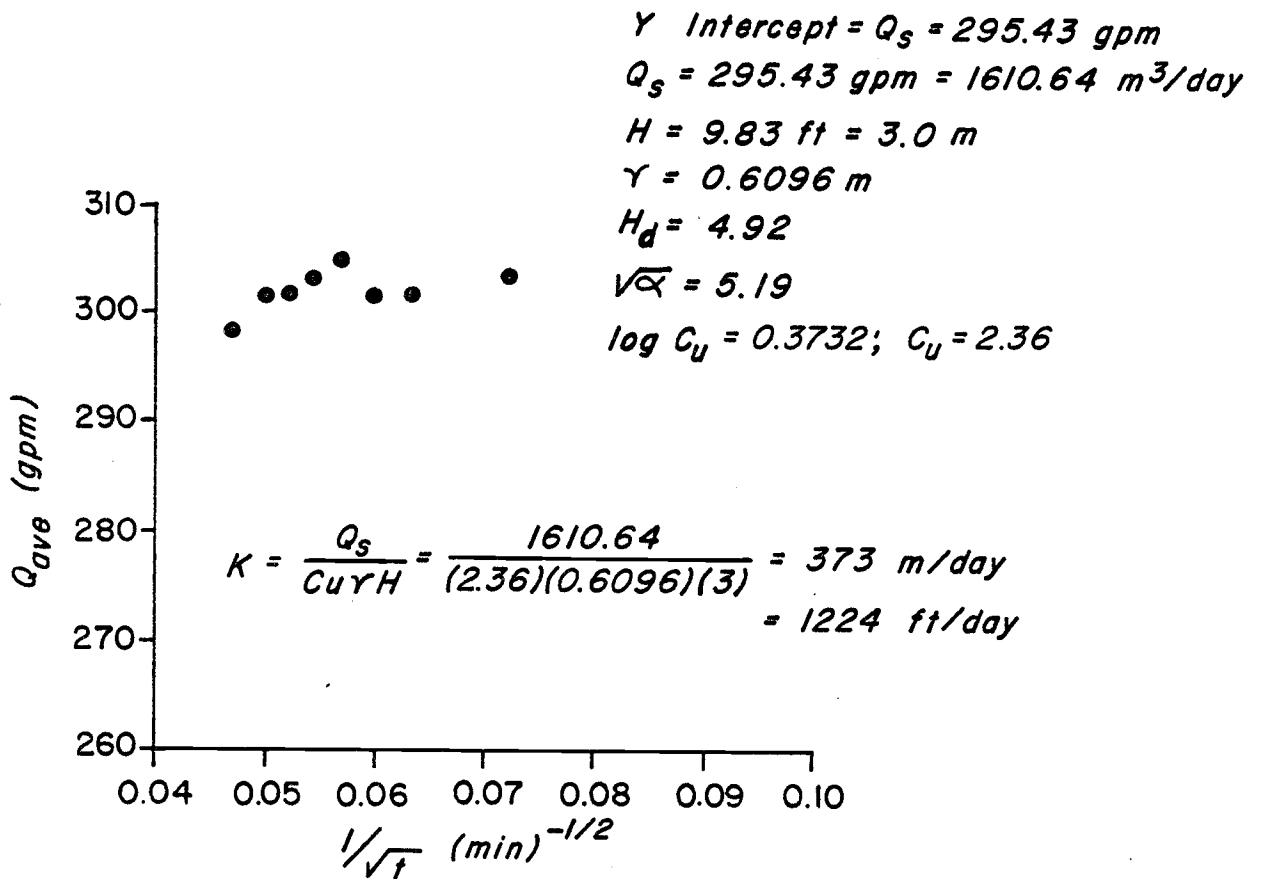


Figure 8. Plot of Flow Rate vs  $t^{-1/2}$  for derivation of Saturated Hydraulic Conductivity.

TABLE 2

Calculated  $K_s$  Values

<u>Dry Well Test No.</u>	<u><math>K_s</math></u>
1	1520 ft/day
2	934 ft/day
3	1496 ft/day
4	1547 ft/day
5	1327 ft/day
7	1224 ft/day
Mean $K_s$ Value:	1312 ft/day

Step 1: Obtain value for  $\alpha$  from semilog plot of  $K_r$  vs  $\Psi$  (see Figure 7). Here  $\sqrt{\alpha} = 5.19$ .

Step 2: Construct a graph of average flow rate vs  $t^{-1/2}$ , from constant head borehole infiltration test data. Table 1 shows the data used to construct the plot shown in Figure 8, a section of data over which head standing in the borehole was relatively constant. Values for  $t^{-1/2}$  are then plotted against the measured flow rate. Linear regression is then used to locate y - intercept to obtain  $Q_s$ , here 1610.6 cubic meters per day.

Step 3: Apply formula and solve for  $K_s$ , saturated by hydraulic conductivity. In this case, using values recorded in Figure 8,

$$\begin{aligned} \log C_u &= (0.658)\log(4.92) - (0.238)(5.19) - (0.398)\log(3) + 1.343 \\ &= 0.3732 : C_u = 2.36 \end{aligned}$$

$$\text{and } K_s = \frac{1610.64 \text{ m}^3/\text{day}}{(2.36)(0.6096 \text{ m})(3 \text{ m})} = 373 \text{ m/day} = 1224 \text{ ft/day}.$$

Table 2 shows the results of this calculation for data from each of the six tests. The variation in calculated  $K_s$  values may be attributed to variations in the amount of entrapped air resulting from the different infiltration rates used and/or varying amounts of fine sediments introduced into the well and surrounding media over time. Variations of this sort commonly lead to differences in  $K_s$  calculated for the same locality of an order of magnitude or more (Neuman, 1984). In light of these facts, the span of  $K_s$  values shown in Table 2 is quite reasonable. A mean value of 1312 ft/day was taken as the best estimate for computational purposes and used in the model.

A check for this value was provided by a  $K_s$  value derived from velocity calculations for laterally moving perched water, derived from neutron log data from a nearby access well (Wilson, 1983, p. 25). Application of the formula

$$K_s = n \bar{v} \left[ \frac{dh}{dl} \right]^{-1}$$

$n$  = medium porosity

$\bar{v}$  = average flow velocity

(After Freeze and  
Cherry, 1979,  
p. 71).

$\left[ \frac{dh}{dl} \right]^{-1}$  = inverse hydraulic gradient

yielded a  $K_s$  value of 1134 ft/day, one considered to be in good agreement with the field test values.

## 2. Pressure Head as Function of Water Content

Using a soil sample obtained from the excavation site of the dry well at the WRRRC Field Lab, taken as representative of the alluvium in which the dry well is set, measurements of volumetric soil water content  $\theta$  corresponding to different applied suction values were obtained at the University of Arizona Soil and Water Testing Laboratory using a porous pressure plate apparatus. From these values, a continuous curve for  $\Psi$  vs  $\theta$  was derived (see Figure 9a).

## 3. Unsaturated Hydraulic Conductivity

A method developed at the U.S. Salinity Laboratory of the U.S. Department of Agriculture for the derivation of the relative hydraulic conductivity ( $K_r$ ), giving the ratio of measured to saturated hydraulic conductivity at various levels of water content, from a knowledge of the  $\Psi$  vs  $\theta$ , or soil moisture retention curve just described, was employed in this study. This method relies on a non-linear least squares curve matching technique to derive an analytical expression for  $\Psi(\theta)$  which is checked against experimental data, then transformed by another analytical model into a tabulation of  $K_r$  vs  $\Psi$  values (Genuchten, 1980). The  $K_r$  vs  $\theta$  curve is then derived via interpolation from this table of values and the original  $\Psi$  vs  $\theta$  curve (see Figure 9b). Though still relatively new, this method has by now gained widespread acclaim by the scientific community, not only for its accuracy, but for its replacement of the alternative costly and tedious laboratory method for obtaining the same data.

Since no samples of the soil comprising the perching layer for



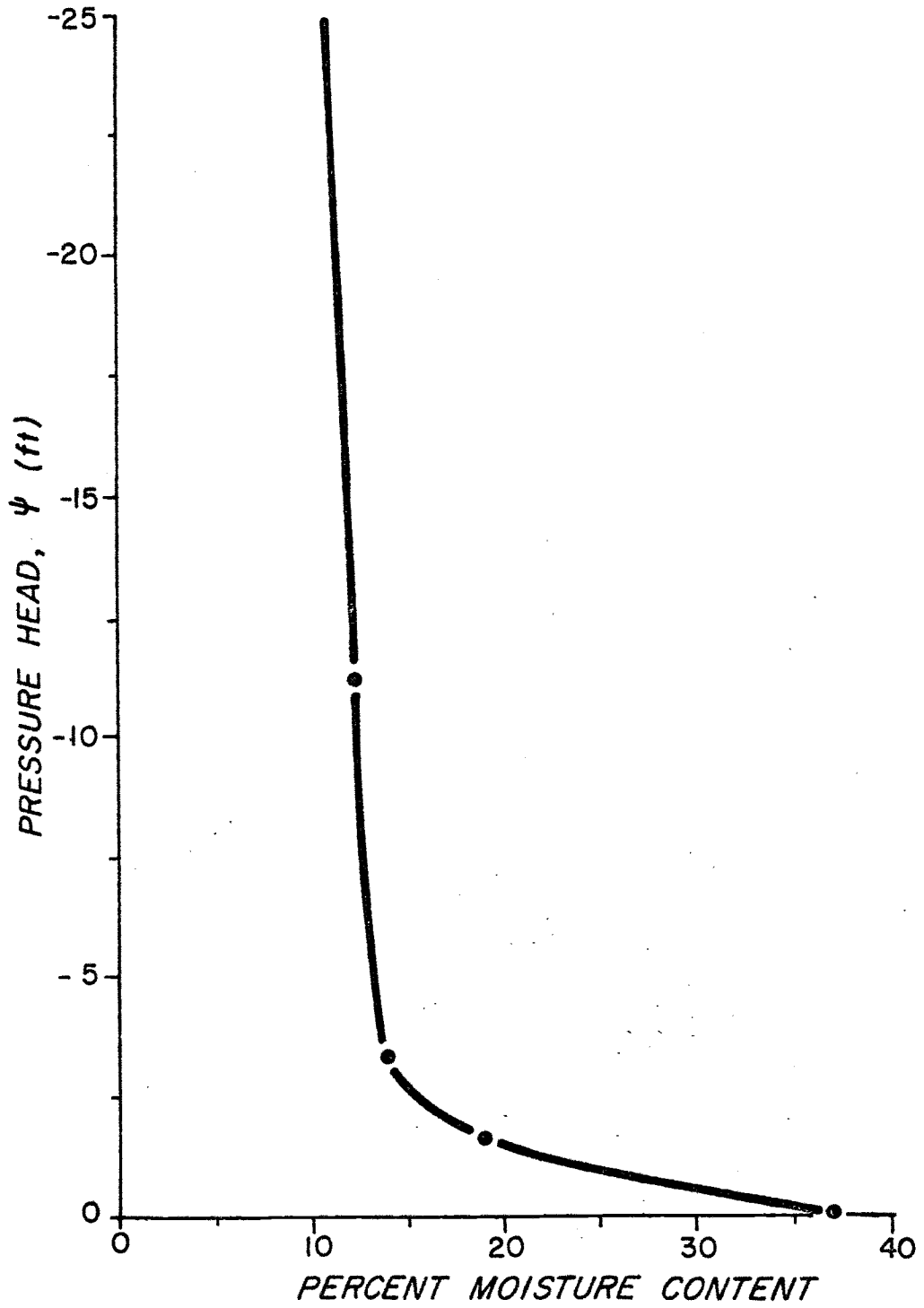


Figure 9a. Experimentally Derived  $\Psi$  vs  $\theta$  Curve.

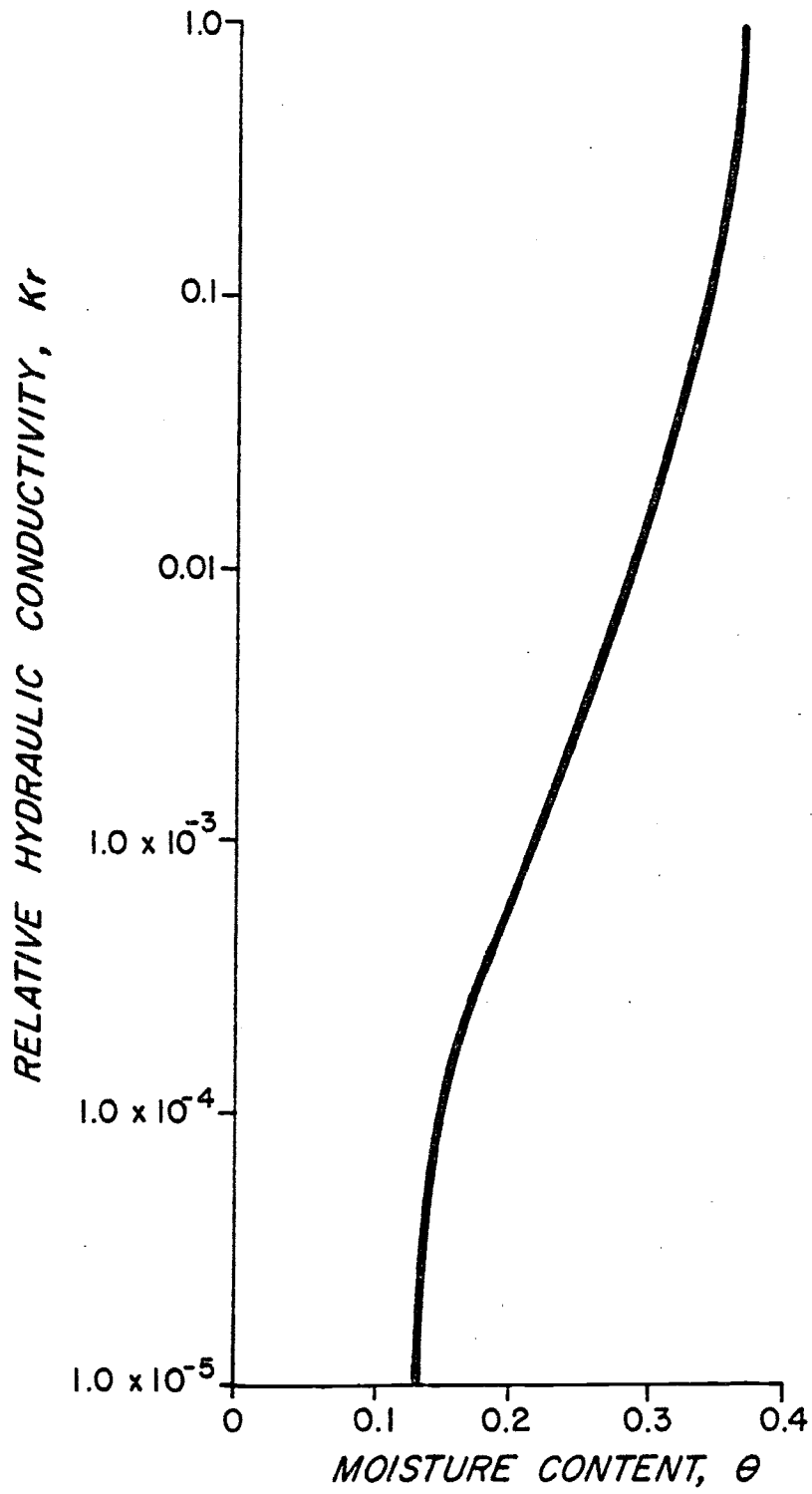


Figure 9b.  $K_r$  vs  $\theta$  Curve for Material 1 (alluvium).

TABLE 3a

Moisture Retention Data for Material 2

Pressure Head ( $-\Psi$ )	vs	Water Content ( $\theta$ )
$-\Psi(\text{Ft. H}_2\text{O})$		$\theta(\%)$
1.00x10 <sup>-2</sup>		35.70
3.00		35.55
8.00		35.50
1.50x10 <sup>-1</sup>		35.35
2.50		35.20
3.00		35.15
3.50		35.05
3.80		35.00
4.00		34.95
4.20		34.90
4.50		34.80
4.70		34.70
4.80		34.50
4.90		34.30
5.00		34.15
5.20		33.30
5.40		31.60
5.60		27.50
6.00		16.40
6.20		13.90
6.40		11.60
6.60		9.90
6.80		8.75
7.00		7.80
7.40		6.30
7.60		5.80
7.80		5.20
8.00		4.90
8.40		4.35
8.60		4.20
8.80		4.00
9.00		3.85
9.40		3.70
9.80		3.60
1.00x10 <sup>0</sup>		3.50
5.00		2.70
1.00x10 <sup>1</sup>		2.35
6.00		1.40
1.00x10 <sup>2</sup>		1.05
6.80		0.00

TABLE 3b

Relative Hydraulic Conductivity Data for Material 2

Conductivity/ Sat. Cond. ( $K_r$ )		vs	Water Content ( $\theta$ )	
$K_r$			$K_r$	$\theta(\%)$
0.00			$3.30 \times 10^{-1}$	25.40
$1.00 \times 10^{-3}$			3.50	25.80
1.50		1.70	3.70	26.15
2.00		1.90	4.00	26.65
3.00		2.35	4.30	27.20
4.00		2.85	4.60	27.80
5.00		3.20	4.90	28.25
6.00		3.60	5.40	29.10
7.00		4.05	5.80	29.70
8.00		4.40	6.40	30.55
9.00		4.80	7.00	31.55
$1.00 \times 10^{-2}$		5.10	7.60	32.50
1.20		5.85	8.00	33.20
1.40		6.50	8.40	33.75
1.60		7.15	9.20	35.05
1.70		7.55	9.60	35.60
1.80		7.90	$1.00 \times 10^0$	36.40
2.00		8.45		
2.40		9.80		
2.60		10.45		
2.80		11.00		
3.00		11.50		
3.20		12.05		
3.70		13.10		
4.00		13.55		
4.30		14.15		
4.70		14.80		
5.00		15.20		
5.40		15.70		
5.60		15.95		
6.00		16.30		
6.40		16.75		
7.00		17.25		
7.40		17.50		
8.00		17.85		
9.00		18.40		
$1.00 \times 10^{-1}$		18.90		
1.20		20.05		
1.30		20.40		
1.50		21.25		
1.70		21.90		
2.00		22.80		
2.40		23.70		
3.00		24.85		

Case 2 at 32 feet were available, indirect methods of analysis were used to obtain the necessary hydraulic properties information for this material. Combining information on soil type and grain size distribution with depth published in a University of Arizona Master's Thesis (Osborne, 1969) with data from neutron moisture logs obtained from previous dry well tests, a soil with similar properties was selected from an expansive catalog of soil types (Muallem, 1976), and its hydraulic properties taken to be representative of the perching layer material. In this manner, values for  $K_s$ ,  $\psi$  vs  $\theta$  and  $K_r$  vs  $\theta$  were all obtained for this second material. Tables 3a and 3b show the values that describe the soil moisture retention curves.

#### Discussion of Results

##### Case 1a: 100 Year Flood: No Vertical Leakage

Figure 10 shows the flow profile as it would appear after the entire runoff from a paved acre had drained into a dry well. As can be seen from Figure 10, the plume would extend approximately 40 feet from the axis of the dry well under these conditions at the time drainage ceased. During dissipation, the plume would then migrate further outward under the influence of gravity drainage, perhaps as far as another 40 feet, depending on the site specific soil hydraulic properties and degree of homogeneity. With these effects being considered in light of the simulation results, a good conservative estimate for maximum lateral migration of the plume from a 100-year storm event under these "worst case" conditions would be roughly 100 feet.

##### Case 1b: 100-Year Flood with Vertical Leakage

Figure 11 shows the predicted flow profile for the same flood under the more realistic conditions of the perching layer being composed of material having a considerably lower, but still positive, permeability than that of the overlying alluvium. The figure shows the flow profile after the entirety of the storm runoff has been drained. Here the

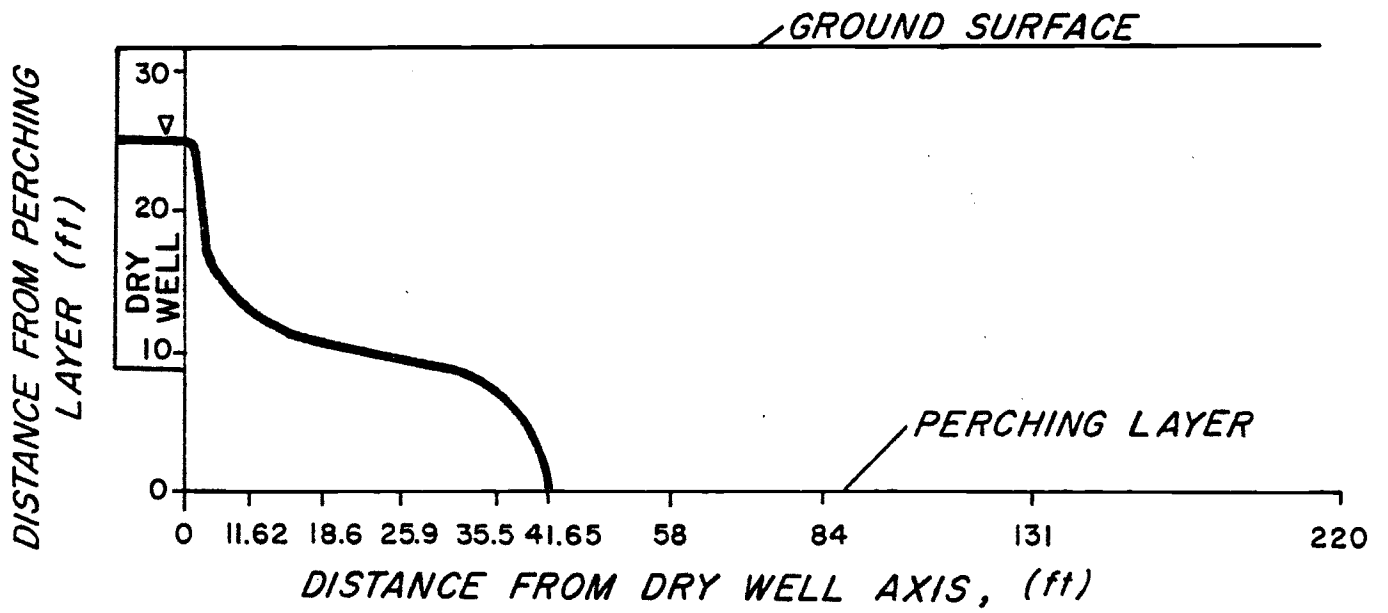


Figure 10. Flow Profile for Case 1a.

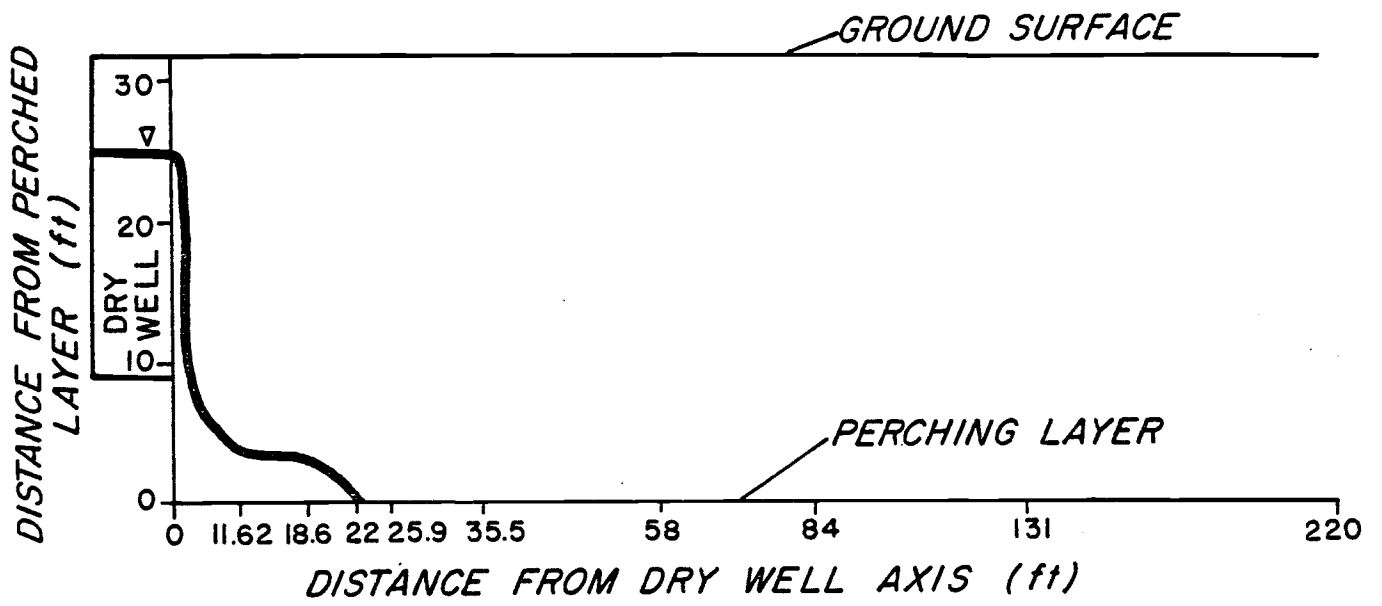


Figure 11. Flow Profile for Case 1b.

effects of vertical drainage sharply reduce the extent of lateral migration. In this case the plume has migrated approximately 25 feet from the well, and would most likely not migrate much further under gravity drainage after the influx of storm water has stopped. In the absence of a wholly impermeable or only slightly permeable perching layer, a good conservative estimate for maximum lateral migration of the drainage plume from a 100-year flood would be roughly 50 feet.

#### Case 2a: Sustained Drainage: No Leakage

This simulation was made again assuming the worst case of an impervious perching layer. Figures 12a-12c show progressive flow profiles at the end of 4.36, 9.11 (Figure 12a), 15.24 (Figure 12b) and 27.22 (Figure 12c) hours, respectively. At this last time interval the outer flow boundary of 680 feet for the simulation grid was reached and no more scientifically accurate predictions based on this simulation can be made beyond this point. Table 3 shows the estimated cumulative flow into the system at various time levels. Judging from these cumulative inflow values and the corresponding flow profiles shown in Figures 12a-c, an approximation of the extent of lateral migration for various expected amounts of total runoff can be obtained for this worst possible case flow regime.

#### Case 2b: Sustained Drainage with Leakage

A more realistic estimate of lateral migration from a dry well under conditions of long-term drainage could be obtained from a simulation where vertical drainage through the perching layer is considered. Unfortunately, due to the massive amounts of computer storage required to perform this simulation, and the great expense involved, this simulation has not been performed. At this time, however, the simulation will be performed and the results published in a University of Arizona Master's thesis by the author within the year.



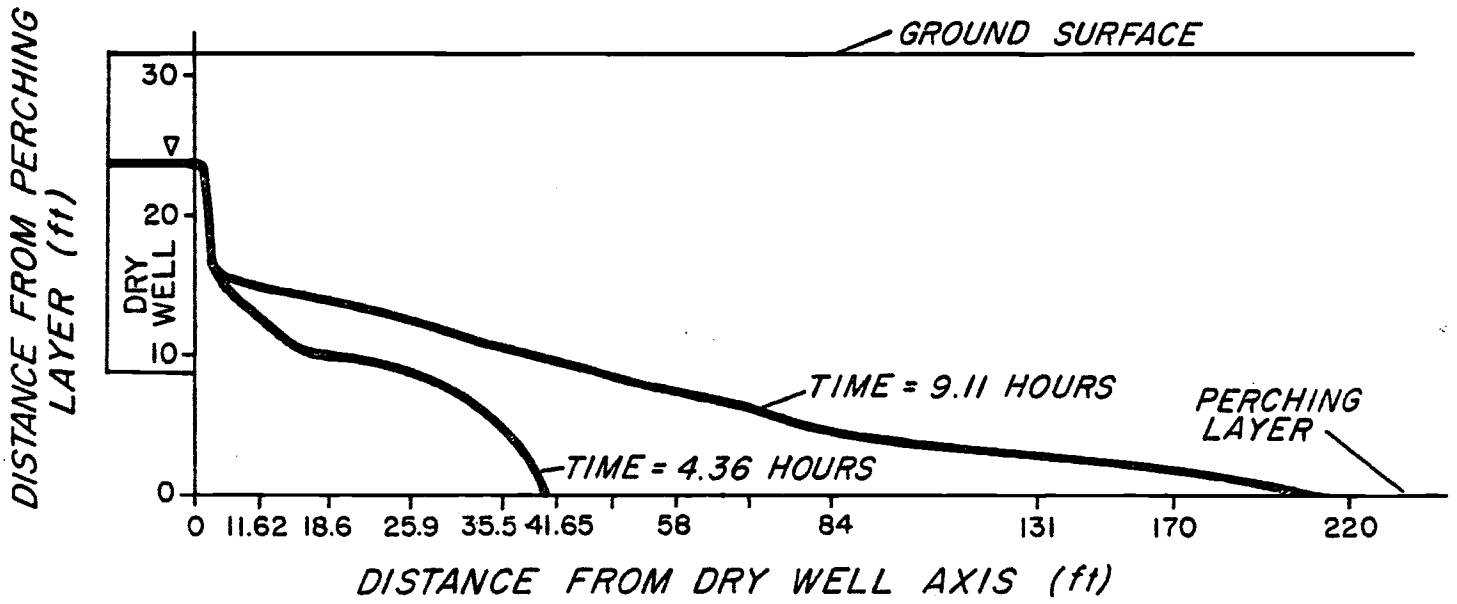


Figure 12a. Flow Profile for Case 2a.

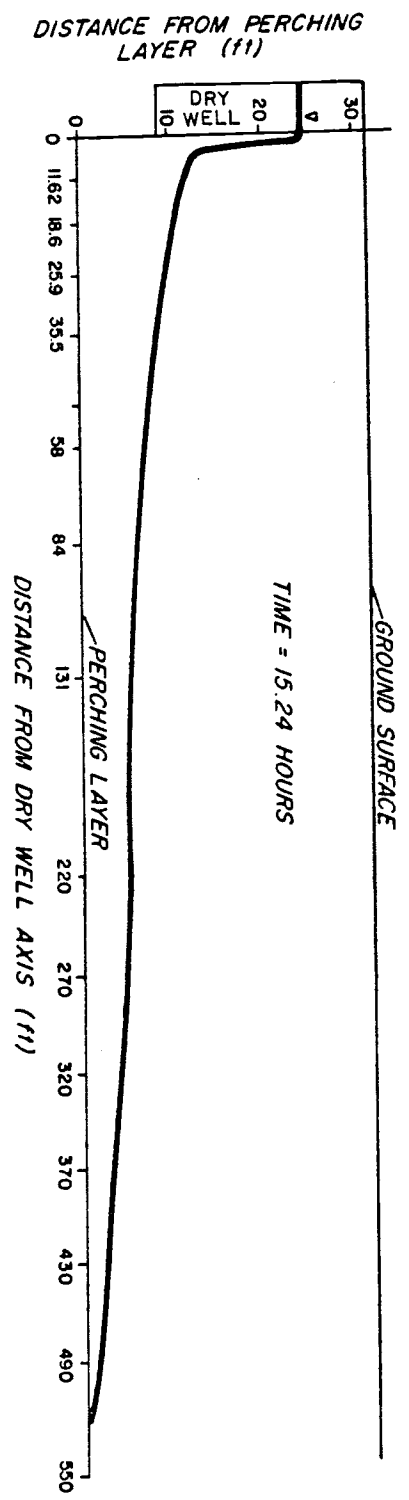


Figure 12b. Flow Profile for Case 2a.

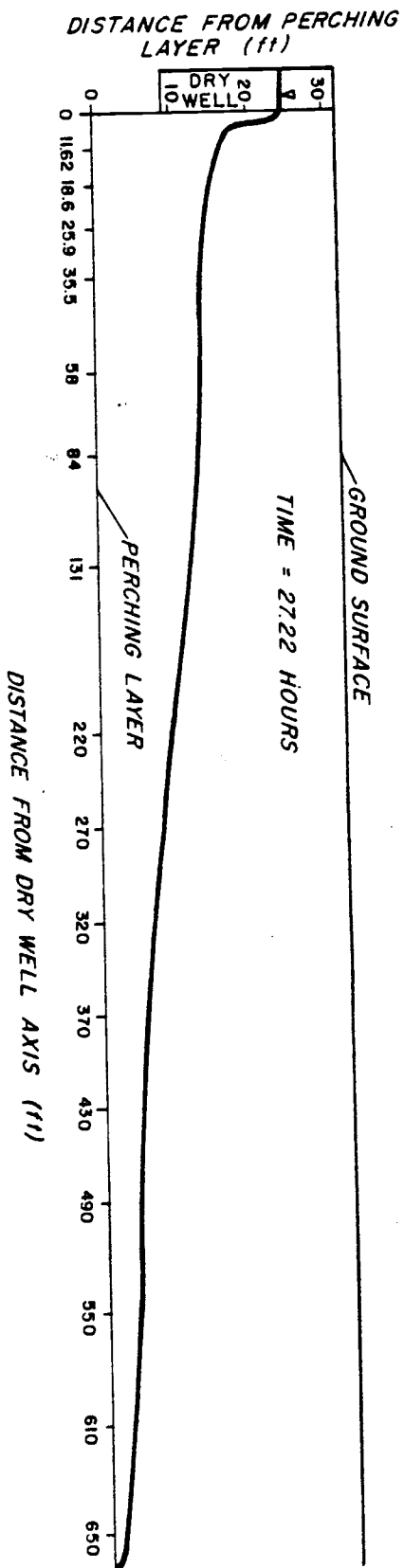


Figure 12c. Flow Profile for Case 2a.

TABLE 4

Cumulative Inflow Data

<u>Time After Start (Hours)</u>	<u>Cumulative Inflow (Cubic Feet)</u>
4.02	7,236.0
4.36	7,848.0
4.78	8,604.0
5.31	9,558.0
5.96	10,728.0
6.79	12,221.8
7.82	14,075.6
9.11	16,393.1
10.72	19,289.9
12.73	22,910.9
15.24	27,437.4
18.38	33,094.8
22.31	40,167.0
27.22	49,006.8

### Conclusions & Recommendations

Judging from the results of this extensive study, the problem of ground water pollution via water well bore leakage due to use of dry wells to dispose of localized storm runoff can be safely avoided by placing all dry wells a minimum distance of 100 feet in any direction from any water well penetrating to the aquifer, provided that the design rule of one Max Well Type III dry well per paved acre specified by the manufacturer is abided by. Depending on the volume of water to be disposed of under static drainage conditions the design placement of dry wells may vary. The results shown in Table 3 may serve as a guideline. It should be kept in mind that these results assume the existence of an impermeable perching layer, and thereby represent a worst possible case. In the absence of such an impermeable stratum, lateral migration will be considerably less.

### Sources

1. Dietrich, Richard V. and Skinner, Brian J., Rocks and Rock Minerals, Wiley and Sons, New York, 1979.
2. Percious, Donald J., Aquifer Dispersivity by Recharge - Discharge of a Fluorescent Dye Tracer Through a Single Well, University of Arizona Master's Thesis, 1969.
3. U.S. Department of Interior, Ground Water Manual, Bureau of Reclamation Technical Publication, 1977.
4. Wilson, L.G., and Schmidt, K.D., Monitoring Perched Ground Water in the Vadose Zone, American Water Resources Association: Reprint, 1978.

### References

1. Campbell, Michael D., and Lehr, Jay H., Water Well Technology, McGraw-Hill, 1973.
2. DeTommaso, S.C., McGuckin Drilling, Inc., Phoenix, Arizona, June 1984. Personal Communication.
3. Dunne, Thomas and Leopold, Luna, Water in Environmental Planning, Freeman and Co., San Francisco, 1978.
4. Freeze, Allan R. and Cherry, John A., Groundwater, Prentice-Hall, N.J., 1979.
5. Genuchten, Rien Van, "Calculating Unsaturated Hydraulic Conductivity with a Closed Form Analytical Model," U.S. Salinity Laboratory, USDA, Riverside, CA, 1978.
6. Heckman, Shirley, Hydrologist, Hargis and Associates, Inc., Hydrogeological Consultants, Tucson, Arizona, August 1984. Personal Communication.
7. Mualem, Yechezkel, "A Catalogue of the Hydraulic Properties of Unsaturated Soils," Technion Institute of Technology, Haifa, Israel, 1976.
8. Nelson, James, Cella Barr Associates, Inc., Environmental Engineers, Tucson, Arizona, June 1984. Personal Communication.
9. Neuman, S.P., Professor of Hydrology and Water Resources, University of Arizona, Tucson, May 1984. Personal Communication.
10. Osborne, P.S., Analysis of Well Losses Pertaining to Artificial Recharge, Master's Thesis, University of Arizona, 1969.

References (Continued)

11. Stephens, D.B. and Neuman, S.P., "Analysis of Borehole Infiltration Tests Above the Water Table," University of Arizona Technical Report No. 35, March, 1980.
12. Wilson, L.G., A Case Study of Dry Well Recharge, Research Project Technical Completion Report, U.S. Department of Interior, Sept. 1983.